

**EFFECT OF JUNCTIONAL ADHESION MOLECULE A, JAM-A, ON NON-ALCOHOLIC FATTY LIVER DISEASE, NAFLD**

by  
Laura S. Shankman

A thesis submitted to the Faculty of the University of Delaware in partial fulfillment of the requirements for the Honors Degree of Bachelor of Science in Cellular and Molecular Genetics with Distinction.

Spring 2007

Copyright 2007 Laura S. Shankman  
All Rights Reserved

**EFFECT OF JUNCTIONAL ADHESION MOLECULE A, JAM-A, ON NON-ALCOHOLIC FATTY LIVER DISEASE, NAFLD**

by  
Laura S. Shankman

Approved: \_\_\_\_\_  
Ulhas P. Naik, Ph.D.  
Professor in charge of thesis on behalf of the Advisory Committee

Approved: \_\_\_\_\_  
Li Liao, Ph.D.  
Committee member from the Department of Computer and Information Science

Approved: \_\_\_\_\_  
Jung-Youn Lee, Ph.D.  
Committee member from the Board of Senior Thesis Readers

Approved: \_\_\_\_\_  
John A. Courtright, Ph.D.  
Chair of the University Committee on Student and Faculty Honors; Vice Provost for Academic and International Programs

## **EPIGRAPH**

“Nothing good comes easily  
Sometimes you gotta fight”  
-“Amber” by 311

## **ACKNOWLEDGMENTS**

Thank you to Dr. Ulhas P. Naik for giving me the freedom to explore uncharted areas, especially to Vesselina Cooke for guiding me there. Thanks to everyone in the Naik lab for your emotional support and help directing me when I did not know where to go. I also need to mention the help of Dr. Li Liao and Roger Craig, whom helped push me to finish my minor in BioInformatics. Dr. Usher helped with my understanding of the liver's function in lipid metabolism, and analyzing my data. Dr. Jung-Youn Lee needs to be thanked for helping me progress as a presenter in the Senior Thesis course. Finally, I need to thank INBRE program and Donald W. Harward Fellows for funding me, and my parents who try to understand my goals in life.

## TABLE OF CONTENTS

<b>LIST OF FIGURES</b> .....	vi
<b>ABSTRACT</b> .....	vii
Chapter	
<b>1 INTRODUCTION</b> .....	1
1.1 Obesity in America .....	1
1.2 Non-alcoholic Fatty Liver Disease .....	1
1.2.1 Pathological Progression.....	3
1.2.1.1 Fatty Liver - Steatosis .....	4
1.2.1.2 Non-alcoholic Steatohepatis.....	6
1.2.1.3 Fibrosis and Cirrohsis of the Liver .....	7
1.2.2 Molecular Pathway of Neutrophil Transmigration .....	8
1.2.2.1 Cytokines .....	10
1.2.2.2 Selectins .....	10
1.2.2.3 $\beta$ -integrins and the Immunoglobulin Superfamily.....	11
1.3 Junctional Adhesion Molecule-A .....	11
1.3.1 JAM-A Function at the Tight Junctions.....	12
1.3.2 JAM-A Function in Leukocyte Transmigration .....	12
<b>2 MATERIALS AND METHODS</b> .....	14
2.1 JAM-A Knock Out Mice .....	14
2.2 Experimental Diets.....	14
2.3 Weekly Observance .....	15
2.4 Blood Sample Collection .....	15
2.4.1 Total Cholesterol.....	15
2.4.2 HDL Cholesterol.....	16
2.4.3 LDL Cholesterol .....	16
2.4.4 Total Triglycerides.....	17
2.5 Histology.....	17
2.5.1 Dissection and Sectioning.....	18
2.5.1.1 Hemotoxylin and Eosin Stain.....	18
2.5.1.2 Masson's Trichrome Stain.....	19
2.5.1.3 Oil Red O Stain.....	19
2.6 Dynamic Database .....	20
<b>3 RESULTS</b> .....	21
<b>4 DISCUSSION</b> .....	35
<b>REFERENCES</b> .....	41

## LIST OF FIGURES

<b>Figure 1: Consequences of Visceral Fat Accumulation</b> .....	2
<b>Figure 2: Progression of Non-alcoholic Fatty Liver Disease</b> .....	4
<b>Figure 3: Liver-adipose cycle for the storage and metabolism of fatty acids</b> .....	5
<b>Figure 4: Representative Microvascular and Macrovascular Images</b> .....	6
<b>Figure 5: Stages of Fibrosis</b> .....	8
<b>Figure 6: Steps of Neutrophil Extravasation During Inflammation</b> .....	9
<b>Figure 7: Genetic Construct of JAM-A (-/-) Mouse</b> .....	14
<b>Figure 8: Total Weight Gain Over Time – Intragroup</b> .....	22
<b>Figure 9: Total Weight Gain Over Time - Intergroup</b> .....	23
<b>Figure 10: Percent Weight Gain Over Time</b> .....	23
<b>Figure 11: Percent Weight Gain as a Function of Sex and Diet</b> .....	24
<b>Figure 12: Total Cholesterol Levels</b> .....	26
<b>Figure 13: HDL-Cholesterol Levels</b> .....	26
<b>Figure 14: LDL-Cholesterol Levels</b> .....	27
<b>Figure 15: Total Triglyceride Levels</b> .....	27
<b>Figure 16: Physiological Reaction to Diets</b> .....	28
<b>Figure 17: Organ Weights as a Percentage of the Total Body Weight</b> .....	30
<b>Figure 18: Hepatitis of Livers – 100X</b> .....	31
<b>Figure 19: Hepatitis of Livers – 400X</b> .....	32
<b>Figure 20: Histology of Adipocytes Stained with H&amp;E – 100X</b> .....	32
<b>Figure 21: Histology of Adipocytes Stained with Oil Red O – 100X</b> .....	34

## ABSTRACT

In America, obesity is one of the fastest growing conditions with an estimated 30% of American adults diagnosed with clinical obesity. There are a manifold of diseases and conditions that stem from obesity, such as, atherosclerosis, type II diabetes, non-alcoholic fatty liver disease (NAFLD), and others. Here we relate the growing concern of excessive weight gain to the function of junction adhesion molecule-A (JAM-A) on NAFLD.

To understand the relation between this junction adhesion molecule and NAFLD, JAM-A (-/-) and JAM-A (+/+) mice were exposed to either a high fat or a low fat diet for 25 weeks. Relative dietary effects were tracked via weight gain and blood cholesterol levels. Progression of NAFLD was characterized by staining liver sections with Masson's Trichrome. The high fat diet resulted in a significant weight gain in JAM-A (-/-) mice, as well as, elevated blood cholesterol levels. However, instances of macrovascular steatosis were highest in JAM-A (+/+) fed a high fat diet. Conversely, JAM-A (-/-) fed high fat diet had increased adipocyte diameters.

Lipid accumulation in the liver causes inflammation and leads to neutrophil mediated steatosis, a cause of NAFLD. In this paper we report that JAM-A: i) maintains tight junctions preventing excessive lipids from entering the adipocytes or liver, ii) plays a role in neutrophil extravasation that leads to increased steatosis of the liver, and iii) plays a role in macrophage-induced steatosis of the fat pads.

## **Chapter 1**

### **INTRODUCTION**

#### **1.1 Obesity in America**

Obesity is one of the fastest growing diseases among Americans today with an estimated 30% of the adult population categorized as clinically obese (1). Deep-fried fatty foods often cost less and taste better than healthy alternatives, giving people little reason to eat healthy. However, obesity is linked to many diseases such as adult onset of diabetes, which afflicts an estimated 18.2 million Americans and is the cause of approximately one in every seven dollars spent on health care (2). A study headed by Dr. Mark A. Pereira found that eating fast food twice a week led to an additional weight gain of ten pounds a year and increased the risk of prediabetes two-fold (2). Therefore, not only are we eating ourselves to death, we are spending our life savings paying for the consequences of doing so.

#### **1.2 Non-alcoholic Fatty Liver Disease**

The liver is the largest gland in the body and plays a central role in metabolic homeostasis. Some of the functions of the liver include uptake, storage and controlled release of nutrients such as lipids; synthesis of plasma proteins, lipoproteins, and phospholipids; digestion and absorption of fats; and degradation and detoxification of endogenous and exogenous materials (3). When individuals store large amounts of

excess fat, especially visceral fat, a cascade of factors lead to liver malfunction and potentially death (Figure 1) (4).

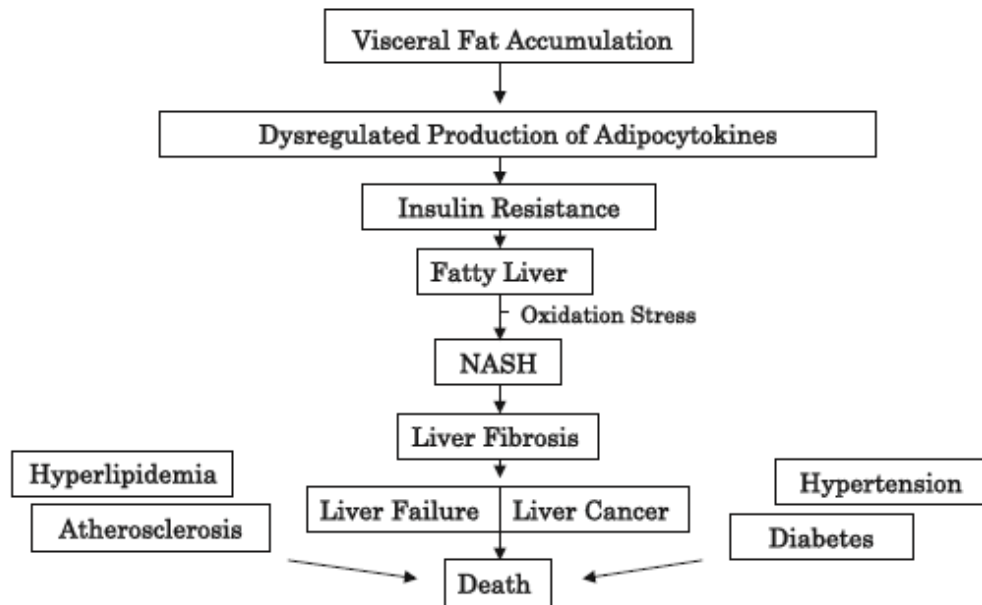


**Figure 1: Consequences of Visceral Fat Accumulation.** A simplified understanding of the cascade of events leading toward late stage NAFLD (NASH & Fibrosis). Also listed are several other diseases that lead to the same outcome (4).

One obesity related disease, non-alcoholic fatty liver disease (NAFLD), recently entered the arena of serious health conditions associated with obesity. Recent reports show that 15-20% of all obese individuals have some form of NAFLD. In addition to obesity, individuals with diabetes, hyperlipidemia, and a variety of other conditions contribute to a total of 15-33% of all Americans having some form of NAFLD. End stage NAFLD is the cause of 4-10% of liver transplants each year (5-8). Not yet known to be the cause of a high body mass index, or a symptom, NAFLD

recorded occurrences are increasing at an alarming pace. NAFLD is also associated with hyperlipidemia, diabetes, and sudden weight gain.

### **1.2.1 Pathological Progression**

NAFLD encompasses diseases such as liver steatosis, a swelling of the liver; non-alcoholic steatohepatitis (NASH), an inflammation of the liver caused by large fat deposits within the liver that damages liver cells (hepatocytes); and cirrhosis of the liver (Figure 2) (9). Risk factors associated with the development of NAFLD include: hyperlipidemia; high body mass index (BMI); rapid weight gain or loss; starvation; prolonged intravenous feeding; use of steroids or estrogen; and gastrointestinal surgery. Symptoms of NAFLD include elevated alanine transaminase (ALT) and aminotransferase (AST). However, one should look into NAFLD if they suffer from type II diabetes, obesity, or hyperlipidemia, because these diseases are often associated with NAFLD (10, 11). Due to the regenerative capabilities of the liver, most stages of NAFLD can be reversed with slow progressive weight loss and exercise; however, not all instances are environmentally influenced (6). If the disease is not caught and corrected in time, it will progressively become worse, and eventually, curable only through transplantation.

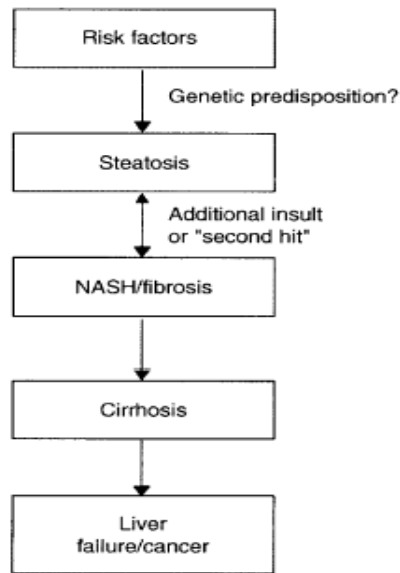


**Figure 2: Progression of Non-alcoholic Fatty Liver Disease (12).**

### 1.2.1.1 Fatty Liver - Steatosis

Fatty liver is a condition where lipids accumulate in the liver and form lipid droplets. These lipid droplets are primarily made up of triglycerides (13), which barrage the liver from multiple sources. Normally, fatty acids are extracted from the food eaten and enter the blood stream via carrier molecules, either very low density lipoproteins (VLDL) or chylomicrons. From there, the triglycerides are either oxidized and used or esterified and sent to the adipocytes for storage (Figure 3) (3). In addition to normal consumption, hepatocytes will compensate for high blood triglyceride levels by increasing triglyceride uptake, often, more than they can process. Another source of triglycerides are the adipocytes. Adipocytes and hepatocytes shift triglycerides back and forth regularly and, under certain conditions, favor transport to the liver (3).

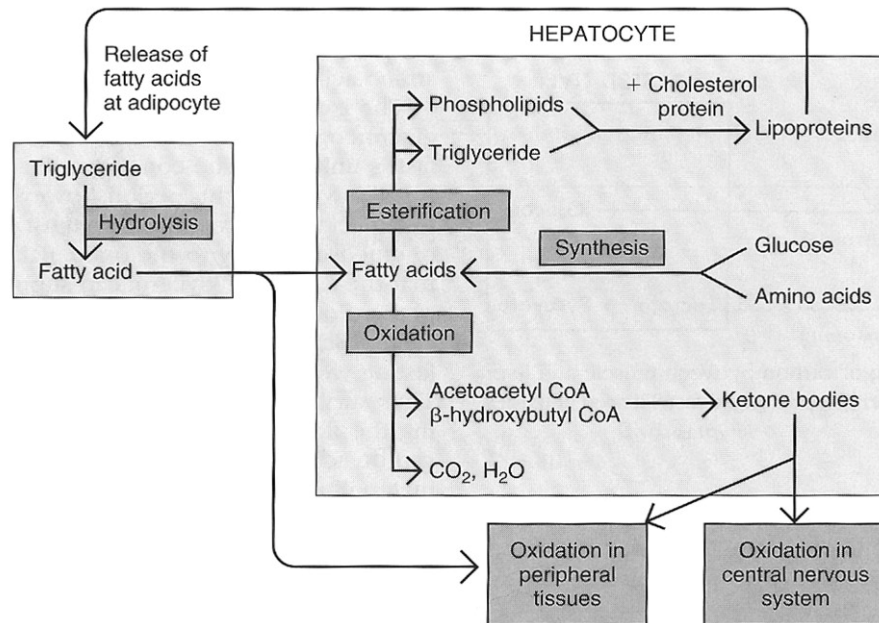


**Figure 3: Liver-adipose cycle for the storage and metabolism of fatty acids (3).**

To be diagnosed as a fatty liver, more than five percent of hepatocytes in the liver must possess: microvascular steatosis; macrovascular steatosis; or a combination of the two. Microvascular steatosis is the accumulation of lipids within the hepatocyte, usually pushing the nuclei proximal to the cell membrane. Defects in mitochondrial function usually cause microvascular steatosis. Macrovascular steatosis, on the other hand, is the accumulation of lipid droplets in the interstitial space and is associated with imbalances in hepatic synthesis and export of lipids (7). Examples of microvascular and macrovascular steatosis can be seen in Figure 4.

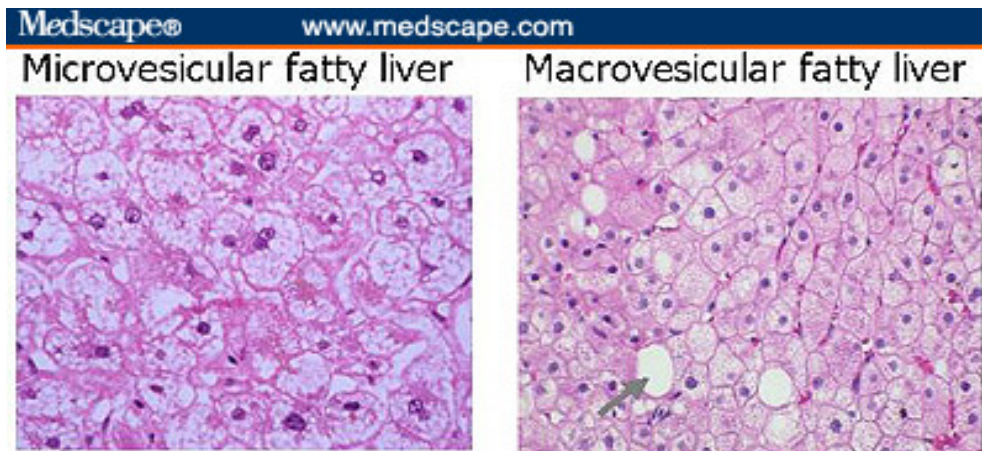


**Figure 4: Representative Microvascular and Macrovascular Images.**

Slides stained with Masson's Trichrome. *Images from: Clinical Perspectives in Gastroenterology*. 2000;129(May/June). Copyright 2000; republished with permission from Elsevier.

#### 1.2.1.2 Non-alcoholic Steatohepatitis

In order to progress from fatty liver to NASH there needs to be a secondary trigger that increases inflammation. Although unclear on precisely what causes the transition, researchers believe that lipid peroxidation is the culprit (11). Several hallmark traits of NASH liver biopsies are: larger amounts of macrosteatosis than microsteatosis; hepatocyte ballooning; parenchymal inflammation; and Mallory bodies (6, 14). Peroxidation initiates a signaling cascade that leads to neutrophil extravasation, discussed further below, that then leads to hepatic apoptosis and damage in areas surrounding the liver damage (15). Neutrophils are phagocytic white blood cells whose normal function involves destroying invading bacteria and clearing necrotic cells in order to prepare for tissue regeneration (15, 16). Risk factors specific to NASH include: Reye's syndrome; fatty liver of pregnancy; rare inherited metabolic diseases; and various toxic syndromes (10).

### **1.2.1.3 Fibrosis and Cirrohsis of the Liver**

Fibrosis begins to develop during the NASH phase of NAFLD. Fibrosis is the build up of collagen in the interstitial space as a defense mechanism against further cell damage (11). Generally, fibrosis will start near zone III of the liver, an area that is poor in oxygen, and contains more catabolic enzymes than zone I. In other words, zone III is undergoing more oxidative stress because it is the main site of lipid metabolism (3, 11). Fibrosis interferes with normal cell function by making transport of molecules from the cell to the blood and vice versa more difficult.

Fibrosis develops into cirrhosis when not treated. As opposed to localizing near the central veins, cirrhosis also develops near the portal arteries. Therefore, cirrhosis disturbs normal function of the liver by blocking blood from entering the liver, inhibiting normal filtration and metabolic functions (3, 11). Also known as end-stage NAFLD, cirrhosis developed through the NAFLD pathway is the cause of 4-10% of liver transplants each year (5). The progression from fibrosis to cirrhosis is shown in Figure 5.

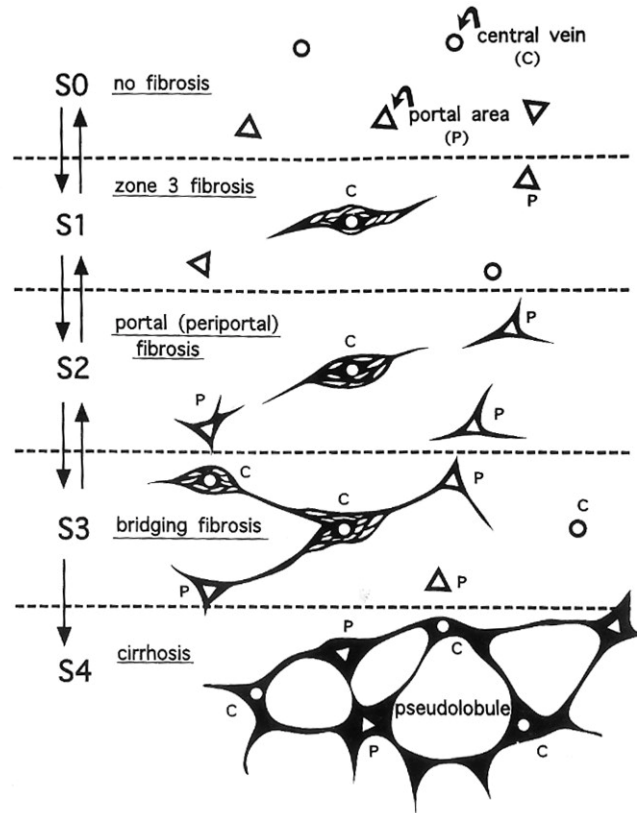


**Figure 5: Stages of Fibrosis.** The progression of fibrosis to cirrhosis caused by non-alcoholic steatohepatitis (11). The liver filters fresh blood from the lungs via the portal areas, as well as, blood cycled through the body from the central veins.

### 1.2.2 Molecular Pathway of Neutrophil Transmigration

White blood cells, known as leukocytes, are critical for protecting the host from invading species and acting as the janitor of the body. Leukocytes identify invading bacteria, viruses, and cells affected by physical trauma through inflammatory signals sent out by distressed cells. Leukocytes will flow through the blood stream until tethered by a selectin. They then roll along the endothelial cell wall until they are activated by an integrin and anchored by an intercellular adhesion molecule (ICAM) (Figure 6). From there various members of the immunoglobulin superfamily (IgSF)

direct the leukocyte through the tight junctions of the endothelial cells toward the site of invasion or damage (17).

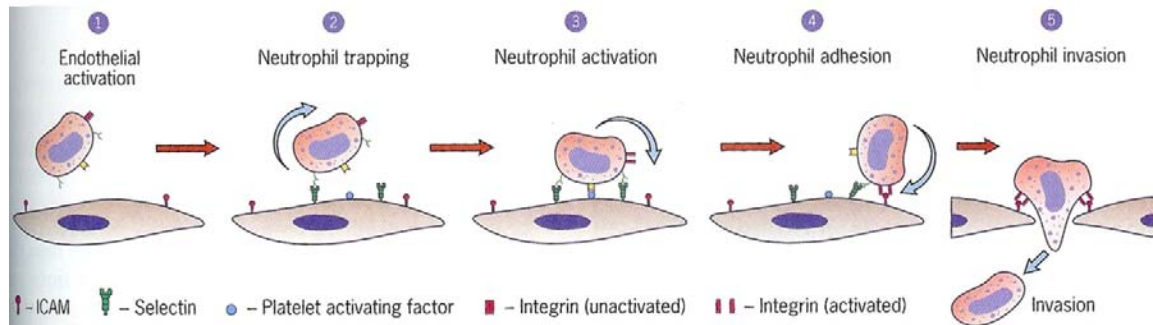


**Figure 6: Steps of Neutrophil Extravasation During Inflammation (18).**

Neutrophils are a subclass of leukocytes that respond to tissue injury, cellular stress, and systemic inflammation. Although the function of neutrophils is important in host defense and removal of cell debris, they can cause additional tissue damage and liver failure if continually activated (19).

High levels of lipid peroxidation products, a symptom of NAFLD, can act as a chemoattractant, bringing neutrophils closer to the hepatocytes. Once a neutrophil comes into contact with a hepatocyte it causes degranulation with release of proteases and formation of reactive oxygen species (ROS). Some of the ROS released include hydrogen peroxide, and hypochlorous acid. These will then diffuse into the cell and cause intracellular oxidant stress and mitochondrial dysfunction, eventually triggering an apoptotic signaling pathway. Necrotic cells will release additional mediators, signaling for more neutrophils, creating a self-amplifying signaling loop for neutrophil extravasation that causes liver damage (15, 16, 19).

### **1.2.2.1 Cytokines**

Cytokines are small secreted molecules that help regulate inflammatory and immune responses. In particular, the CXC chemokines, cytokines with chemotactic function, such as tumor necrosis factor alpha (TNF- $\alpha$ ), interleukin 1 alpha (IL-1 $\alpha$ ), interleukin 1 beta (IL-1 $\beta$ ), cytokine-induced neutrophil chemoattractant (CINC-1), macrophage inflammatory protein-2 (MIP-2), vascular endothelial growth factor (VEGF), and others are responsible for signaling an inflammatory response in the liver. CXC chemokines are released when hepatocytes undergo a lot of metabolic stress, and also during early stages of apoptosis (15, 16, 20).

### **1.2.2.2 Selectins**

Selectins tether neutrophils from the blood causing them to roll along the endothelial cell layer. Released CXC chemokines during inflammation will signal for nearby endothelial cells to activate P- and E-selectins. The selectins cause transient adhesions to circulating neutrophils, slowing their progression and causing them to roll along the endothelial cell layer. The transient adhesion to selectins induces the activation of integrins on the surface of the neutrophil, promoting secure binding to the endothelial cell (18). Sinusoids of the liver do not express E- or P-selectin, therefore, this section of the leukocyte pathway does not occur from the sinusoids to the hepatocytes. However, selectins are expressed and may have a role in the liver post-sinusoidal venules (21).

### 1.2.2.3 $\beta$ -integrins and the Immunoglobulin Superfamily

In response to transient selectin adhesion, the neutrophils will begin to express integrins on their cell surface. Integrins that play a role in neutrophil-endothelial cell adhesion include:  $\beta$ 2-integrins lymphocyte function-associated antigen 1 (LFA-1), very late antigen-4 (VLA-4), Mac-1, and  $\beta$ 1-integrin  $\alpha$ 4 $\beta$ 1 (21-24). Ligands of LFA-1 include members of the immunoglobulin superfamily (IgSF) such as ICAM, and junction adhesion molecule A (JAM-A), whereas, VLA-4 binds to vascular cell adhesion molecule (VCAM) (22, 24). These integrin-IgSF member binding allow for other members of the IgSF to bind and transport the neutrophil to the tight junctions for diapedesis. IgSF molecules believed to be involved in the transport to and through the tight junctions include PECAM-1 and JAM-A (23).

Inhibition of PECAM-1 results in a 90% reduction of leukocyte transmigration *in vitro* (25). Blocking of JAM-A *in vitro* did not result in a decreased diapedesis, however, *in vivo* studies show significant reduction of neutrophil transmigration during ischemia/reperfusion studies. However, sinusoids of the liver do not express PECAM-1 or another related molecule, VE-cadherin. Instead, sinusoids express high levels of ICAM-1 and VCAM-1 which take over the role of PECAM-1 (21).

### 1.3 Junctional Adhesion Molecule-A

JAM-A is a 32 kDa transmembrane protein of the IgSF, similar to the CTX, ESAM, A33, CAR and CLMP. JAM-A has two extracellular Ig loop domains and a

short cytoplasmic domain; also, it localizes in the tight junctions of epithelial and endothelial cells. Several roles of JAM-A include: endothelial cell adhesion and migration, leukocyte transmigration, platelet adhesion, and angiogenesis (26, 27). Recently JAM-A's role in neutrophil transmigration has been a hot topic in many journals.

### **1.3.1 JAM-A Function at the Tight Junctions**

JAM-A localizes in the tight junctions of endothelial and epithelial cells, helping regulate the permeability and stability of the junction, mainly through its ability to homodimerize at the apical part of the lateral membrane (28). JAM-A is also involved in the recruitment of junction adhesion molecules zonula occludens-1 (ZO-1), and occludin (27). JAM-A's position at the apical point of the tight junction allows for involvement with molecule trafficking through the tight junctions of the endothelial cell layer.

### **1.3.2 JAM-A Function in Leukocyte Transmigration**

Members of the IgSF actively participate in leukocyte diapedesis in various organs. During inflammatory events in the liver such as post-ischemia, JAM-A migrates to locations where it is not normally detected, immediately suggesting an important function of JAM-A in leukocyte transmigration (21). Researchers have shown that pro-inflammatory cytokines TNF- $\alpha$  and IFN- $\gamma$  are elevated during neutrophil infiltration suggesting that CXC chemokines either assist neutrophil

diapedesis by removing the JAM-A regulation of the tight junctions, or by assisting in the migration from the endothelial surface to the tight junctions (29).

JAM-A also acts as a ligand for  $\beta$  integrin LFA-1, assisting in adhesion to the endothelial cell layer and movement toward the tight junctions (22, 24). In ischemia-reperfusion (I/R) studies, JAM-A null mice had decreased neutrophil transmigration of 45%, another sign of JAM-A's importance in neutrophil extravasation (21).

In general, when expression of members of the IgSF is reduced, there is a decrease in damaging inflammation (30); however, in an experiment conducted by Khandoga et. al leukocyte diapedesis in the liver was decreased, but adhesion to the endothelial cell layer increased causing more oxidative damage to the liver (21). The exact role of JAM-A in neutrophil diapedesis still remains unclear. However, researchers have established that JAM-A is a player in the complex process of neutrophil transmigration.

## Chapter 2

### MATERIALS AND METHODS

#### 2.1 JAM-A (-/-) Mice

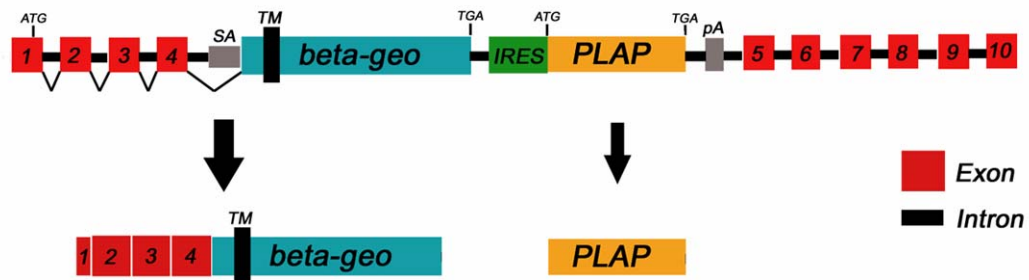


**Figure 6: Genetic Construct of JAM-A (-/-) Mouse.** Genetic construct inserted into the JAM-A gene between the fourth and fifth exons generating a  $\beta$ -galactosidase-JAM-A fusion protein (31).

JAM-A (-/-) mice were used to investigate the *in vivo* effects of JAM-A on NAFLD. Twenty-one age-matched mice, average: 10 weeks old, were divided into four experimental groups.

#### 2.2 Experimental Diets

A low sucrose base pellet feed was used for experimentation: six JAM-A (+/+) mice on a low fat diet, five JAM-A (+/+) mice on a high fat diet, five JAM-A (-/-) mice on a low fat diet, five JAM-A (-/-) mice on a high fat diet. The diets are of the same protein and fat composition listed in Surwit et. al (32) with the vitamin

composition of modified LabDiet® Mouse Diet 5015 with 3000 IU/KG Natural Vitamin E to prevent dermatitis. Low fat diet contained 4.9% (wt/wt) fat, 15.7% (wt/wt) protein, and 73.2% (wt/wt) carbohydrates. The high fat diet contained 35.9% (wt/wt) fat, 20.8% (wt/wt) protein, and 34.3% (wt/wt) carbohydrates.

### **2.3 Weekly Observance**

For twenty-five weeks the mice were weighed weekly in grams to document the progression of the diets. Mice were also inspected for variance in general phenotypic characteristics such as skin condition.

### **2.4 Blood Sample Collection**

Every four weeks the mice were placed on a fourteen-hour fast. At the end of the fast, 400µL of blood was drawn from each mouse via retro-orbital bleeding using a non-coated capillary tube. Blood samples from each experimental group were pooled together in a K<sub>2</sub>EDTA 3.6mg collection tube BD diagnostics. Tubes were then centrifuged at 3000rpm for five minutes in order to separate the plasma from the red blood cells (33). The plasma was then placed in -80°C until enzymatic tests were run.

#### **2.4.1 Total Cholesterol**

Total cholesterol was determined using a Cholesterol E determination kit from Wako Chemicals. From each sample, 20µL of sample were pipetted into 3mL glass

tubes. Then 2mL of color reagent were added to each sample and the samples were incubated for five minutes at 37°C. Absorbance was measured using a spectrophotometer set at 600nm. Total cholesterol content was determined from a standard curve.

#### **2.4.2 HDL Cholesterol**

HDL-cholesterol was determined using a HDL-Cholesterol E determination kit from Wako Chemicals. A 20µL aliquot of sample was mixed with 20µL of precipitating reagent and allowed to react for ten minutes at room temperature. The samples were then centrifuged at 3000rpm for fifteen minutes and the supernatant was isolated. From the supernatant, 5µL of supernatant was mixed with 3mL of color reagent and incubated for five minutes at 37°C. Absorption was measured using a spectrophotometer set at 600nm.

#### **2.4.3 LDL Cholesterol**

LDL-cholesterol was determined using a modified L-Type LDL-C Microtiter procedure kit from Wako Chemicals. From the sample a 6µL aliquot was added to 540µL of reagent I and incubated for five minutes at 37°C. The absorbance was then measured at 600nm. Next, 180µL of reagent II was added to the sample, which was then mixed and incubated at 37°C for five minutes. The absorbance was measured

again at 600nm. In order to determine the LDL content the following equation was used:

$$\text{Final Absorbance} - \text{Initial Absorbance} * (\text{Factor F}) = \text{Final Value}$$

$$\text{Factor F} = (\text{Sample volume} + \text{Reagent I volume}) / (\text{Sample Volume} + \text{Reagent I Volume} + \text{Reagent II volume})$$

Final values were compared to a standard curve to determine the concentration of LDL-cholesterol in the blood.

#### **2.4.4 Total Triglycerides**

Total triglyceride levels were determined using the Serum Triglyceride Determination Kit, method B1, from Sigma Aldrich. One milliliter of triglyceride working reagent was pipetted into each tube. Next, 10 $\mu$ L of sample was added to the working reagent and the samples were incubated for five minutes at 37°C. The absorbance was measured at 540nm and compared to a standard curve.

#### **2.5 Histology**

Transgenic mice used for experimentation were sacrificed via carbon monoxide asphyxiation followed by cervical dislocation.

## **2.5.1 Dissection and Sectioning**

The liver and fat pads were removed from the mouse and weighed. Once the organ was weighed it was placed in 10% formalin pH 7.0, and embedded in paraffin for sectioning. Seven nm sections were prepared using a microtome and placed on slides.

### **2.5.1.1 Hemotoxylin and Eosin Stain**

Hemotoxylin and Eosin staining (H&E) identifies nuclei in blue, cytoplasm in pink, cartilage in dark blue, and blood in bright red. Fat pad sections were stained using an H&E stain to identify the adipocyte cytoplasm near the cell membrane. Slides are deparafinized and rehydrated: two changes of orange oil for ten minutes each; three changes of 100% ethanol for three minutes each; three changes of 95% ethanol for two minutes each; 70% ethanol for two minutes; and rinse in distilled water. Next, they are stained with Harris hematoxylin for ten minutes and rinsed until clear. Then the slides are rinsed in distilled water and placed in acid alcohol for three dips, washed in distilled water, placed in ammonia water for two dips, washed in running water for ten minutes, and placed in 80% ethanol for five minutes. Slides are then placed in eosin solution for four minutes. Finally, the slides were dehydrated: two changes of 95% ethanol for five dips each; two changes of 100% ethanol for five dips each; and three changes of orange oil for ten dips each. Slides are then protected with a coverslip using permount gel mount.

### **2.5.1.2 Masson's Trichrome Stain**

Masson's Trichrome stain identifies nuclei in black; cytoplasm, keratin, and muscle fibers in red; and collagen, mucin in blue. Liver sections were stained with Masson's Trichrome stain to identify any cirrhotic areas. Briefly, slides were deparaffinized and rehydrated before placing in Bouin's fixative overnight at room temperature. Slides are placed in Weigert's iron hematoxylin for ten minutes, rinsed in running water for ten minutes, placed in Beibrich scarlet-acid fuchsin solution for fifteen minutes, and rinsed until clear. Next, slides are placed in phosphomolybdic-phosphotungstic acid solution for fifteen minutes, followed by aniline blue solution for twenty minutes, rinsed, and then placed in 1% acetic water for five minutes. Finally, slides are dehydrated and protected with cover slips mounted using permount.

### **2.5.1.3 Oil Red O Stain**

Oil Red O Stain identifies lipid droplets in bright red and nuclei in blue. An Oil Red O staining protocol modified from F.B. Johnson was used to stain the fat pads and liver to identify accumulation of lipids. Working solution of Oil Red O was prepared by mixing five percent Oil Red O into propane-1,2-diol and placed on a low heat for twenty minutes before filtering through course grade filter paper. The mixture was allowed to sit overnight before being filtered through a Seitz filter with aid of a vacuum. The slides were prepared by deparaffinizing and rehydrating them to deionized water. Next, the slides were placed in the working Oil Red O solution and

allowed to sit for five days. The slides were then differentiated in 85% propane-1,2-diol solution for two minutes and washed in tap water. Slides were then placed in Harris hematoxylin solution for ten minutes, followed by a dip in 1% acid alcohol. Following the acid alcohol, slides were washed in tap water for four minutes, placed in ammonia water, washed in tap water for another four minutes and cover-slipped using a water-based medium.

## **2.6 Dynamic Database**

A dynamic database was incorporated into a web-server using perl script and cgi.pm. Data from a flat file database was hashed and reorganized into arrays. A search engine was then created that included a string search, an AND search, and an OR search option. The AND and OR search options included options acquired from the flat file database: the identification of the photo; the gender of the mouse; the sex of the mouse; the organ viewed; the date of birth of the mouse; the diet; the genotype of the mouse; and the staining used to view the image. Once the search options are submitted, the user is redirected to a new page that includes a table of all the photos matching the search categories. The photo identification column was created to be a clickable hyperlink that sends the viewer to a new webpage. The new page contains the photo of the section, a table describing the photo, and a text box allowing users with the correct password to modify the notes section. The modified database is then saved to a back up file for the main user to view before updating the original database.

## Chapter 3

### RESULTS

The progression of NAFLD is a complicated disease that cannot be accurately studied *in vitro*. Murine model systems are often used for pathophysiological progression of human diseases since they are easily generated and closely resemble the human progression. Most NAFLD studies use obesity prone mice (ob-/ob-), however, the creation of double knockout mice is difficult and time consuming. Therefore, in order to study the natural progression of NAFLD in relation to the presence or absence of JAM-A, we used JAM-A (-/-) mice on a high fat diet designed to induce weight gain.

JAM-A (-/-) and JAM-A (+/+) mice from the JAM-A colony were fed either a high-fat diet containing 35.9% (wt/wt) fat or a low fat diet containing 4.9% (wt/wt) fat *ad libitum*, beginning at ten weeks of age. Body weights were measured once a week in order to track the progression of the diet (Figure 8). Compared to low fat JAM-A (-/-), high fat JAM-A (-/-) mice gained significantly more weight. However, high fat JAM-A (+/+) mice showed no difference in weight gain compared to the low fat JAM-A (+/+) mice (Figure 9).

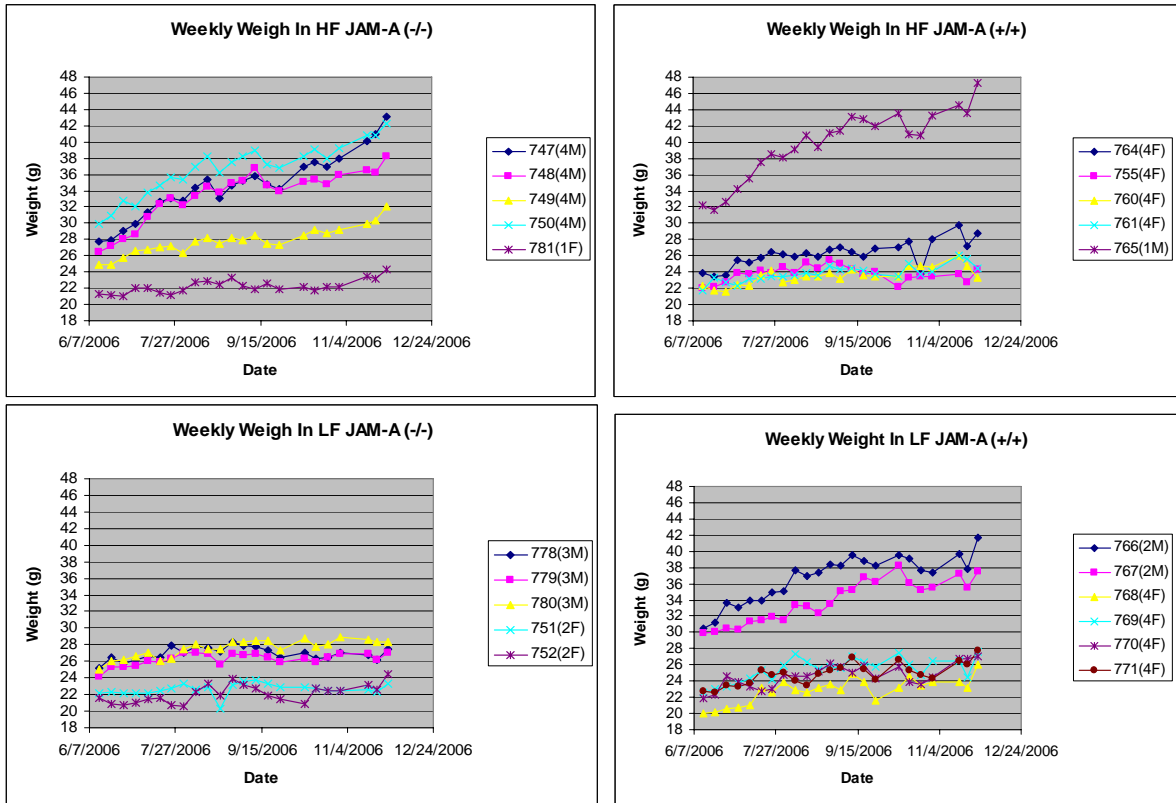


**Figure 8: Total Weight Gain Over Time – Intragroup.** Weekly weights of the mice for the duration of the experiment. The legends indicate the sex of the mouse and the number of mice sharing one cage. From left to right and top to bottom: low fat JAM-A (+/+) mice, low fat JAM-A (-/-) mice, high fat JAM-A (+/+) mice, high fat JAM-A (-/-) mice.

### Total Weight Variation Intergroup

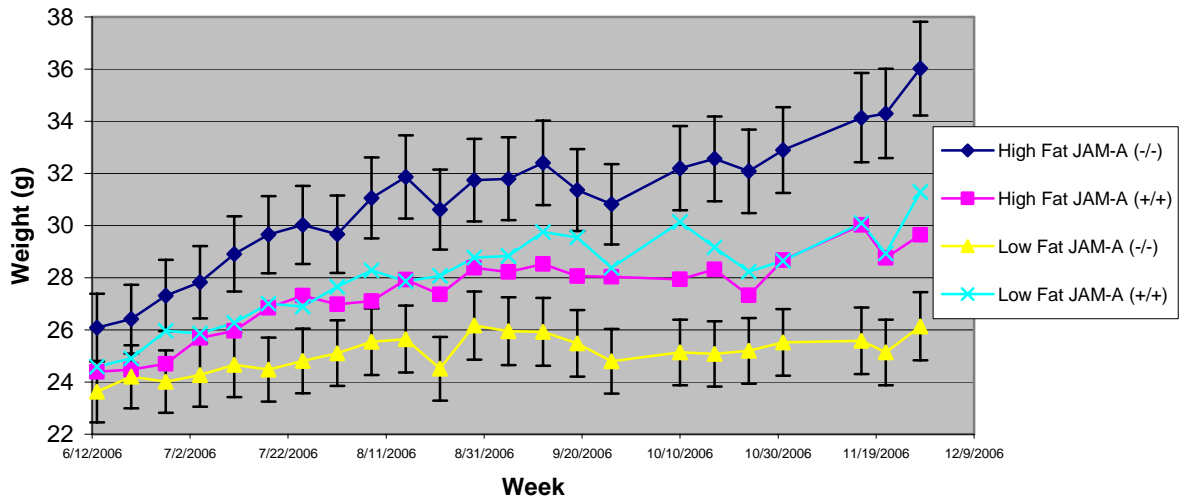


**Figure 9: Total Weight Gain Over Time - Intergroup.** Average weekly weights of the experimental groups for the duration of the experiment. Ninety-five percent confidence shows that high fat (-/-) mice gained more weight than low fat (-/-) mice.

### Total % Weight Variation Intergroup

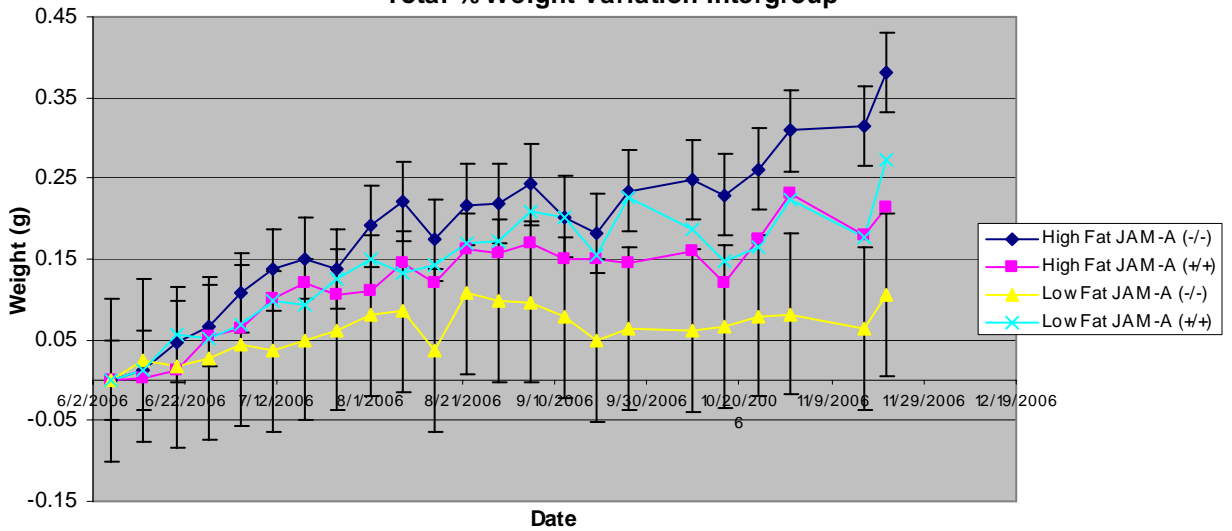


**Figure 10: Percent Weight Gain Over Time.** Average percent weight gained over time per experimental group based on initial body weight  $[(\text{final}-\text{initial})/\text{initial}]$ . Five percent error bars show variance between high fat and low fat JAM-A (-/-) mice.

The data were normalized by calculating the weight gain as a percent of the initial body mass (Figure 10). Trends seen in gross weight gain were also seen in percent weight gain calculations. Data were broken down and analyzed based on the sex of the mouse as well as diet group. Low fat JAM-A (+/+) and low fat JAM-A (-/-) mice showed little to no difference in weight gain between the male and female mice. However, the two high fat diet groups showed a dramatic variance between male and female mice, with male mice gaining over thirty percent more weight than female mice (Figure 11).

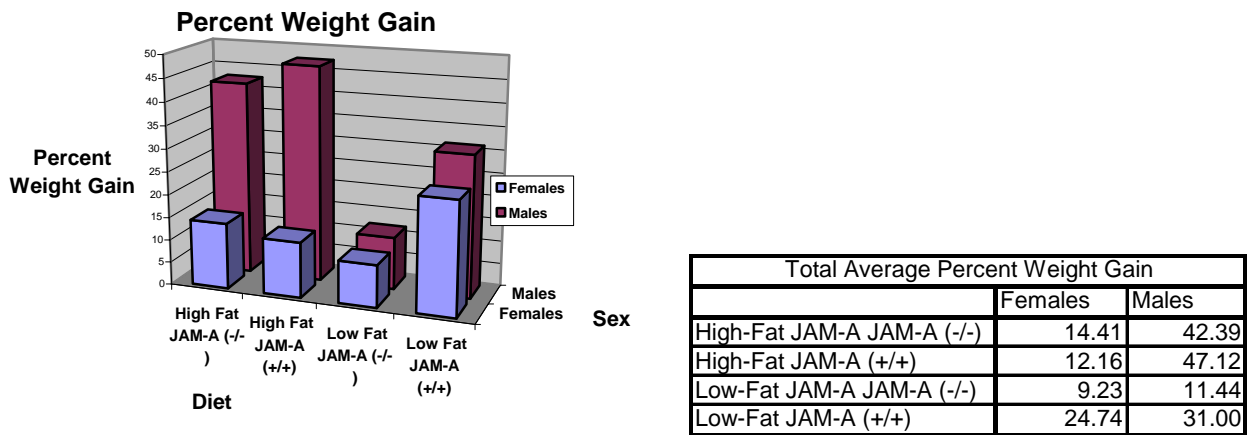


**Figure 11: Percent Weight Gain as a Function of Sex and Diet.** Average percent weight gained over time broken down into experimental group and sex of mouse [(final weight-initial weight)/initial weight]. Left: graphical representation. Right: values of each sub-group.

Another method for tracking diet progression was to monitor cholesterol in the blood plasma. Once a month, the mice were fasted for fourteen hours, after which approximately 400 $\mu$ L of whole blood was drawn from each mouse via retro-orbital bleeding. Blood from mice on the same diet was pooled and centrifuged in order to

collect blood plasma. Total cholesterol, HDL-cholesterol, LDL-cholesterol, and total triglyceride levels were determined from the blood plasma. The control group, low fat JAM-A (+/+) mice, was used to determine the healthy cholesterol levels in the blood (Dr. David Usher: Personal Correspondence). Based on the experimentally derived accepted cholesterol levels, low fat JAM-A (+/+) mice, low fat JAM-A (-/-) mice, and high fat JAM-A (+/+) mice all had normal total cholesterol levels (Figure 12). According to human standards for total cholesterol, the low fat JAM-A (-/-) mice were borderline risk for heart disease, whereas the high fat JAM-A (-/-) mice were in serious risk for heart disease.

Tests for HDL-cholesterol revealed low fat JAM-A (+/+) mice with the lowest amount of HDL-cholesterol followed by low fat JAM-A (-/-) mice, and high fat JAM-A (+/+) mice. Significantly more HDL-cholesterol was found in high fat JAM-A (-/-) mice (Figure 13). Based on low fat JAM-A (+/+) standards, low fat JAM-A (-/-), and high fat JAM-A (+/+) mice were both in the acceptable range. However, high fat JAM-A (-/-) mice fell into the high risk category for LDL-cholesterol (Figure 14). Human standards cannot be considered when examining the levels of HDL- and LDL-cholesterol because humans tend to have lower levels of HDL and higher levels of LDL than mice (Dr. David Usher: Personal Correspondence). Total triglyceride levels varied for all test groups (Figure 15).

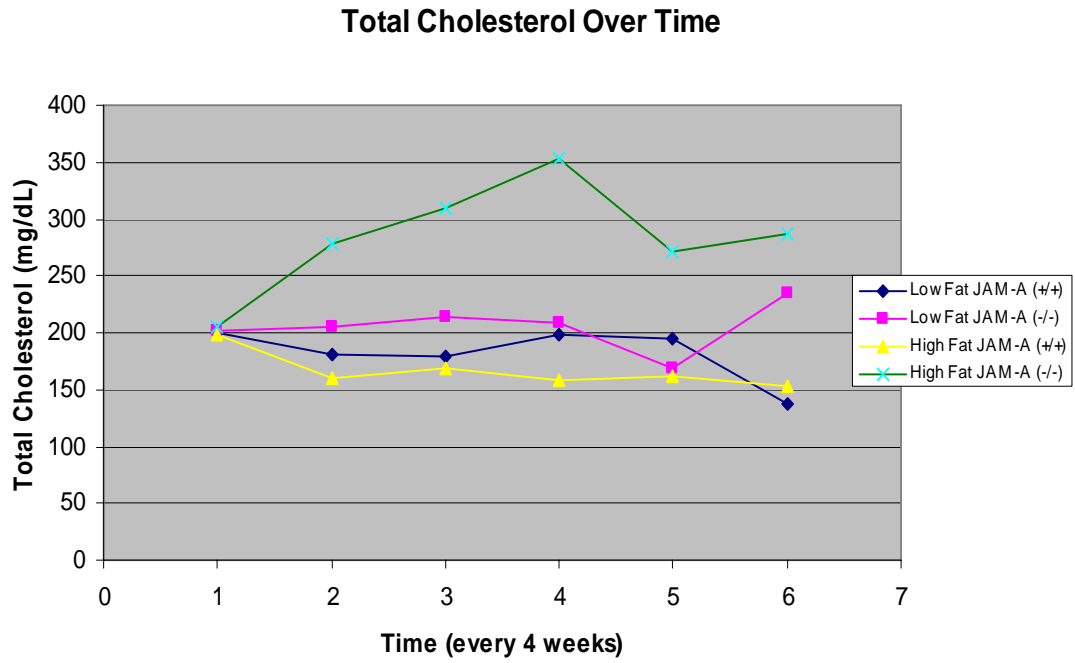


**Figure 12: Total Cholesterol Levels.** Total cholesterol levels derived from blood plasma samples taken once every four weeks via retro-orbital bleeding.

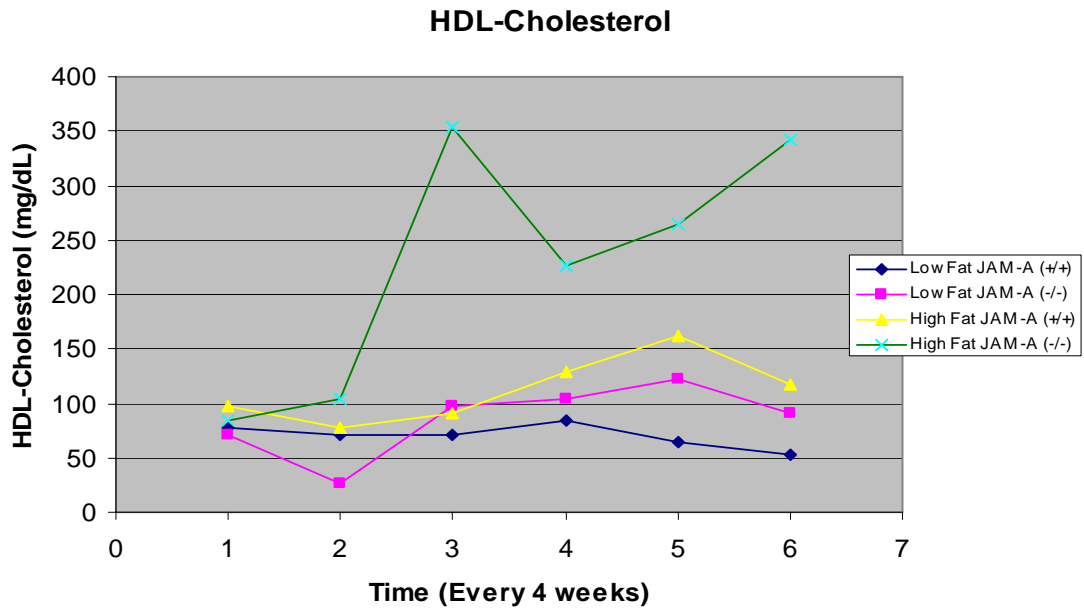


**Figure 13: HDL-Cholesterol Levels.** HDL-cholesterol levels derived from blood plasma samples taken once every four weeks via retro-orbital bleeding.

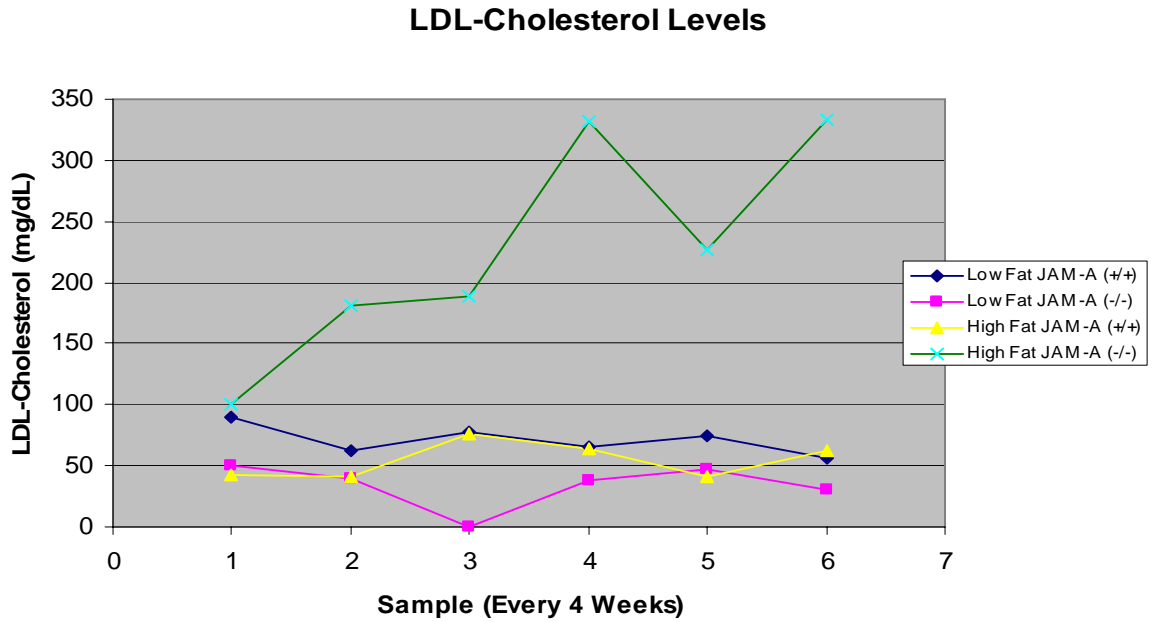


**Figure 14: LDL-Cholesterol Levels.** LDL-cholesterol levels derived from blood plasma samples taken once every four weeks via retro-orbital bleeding.

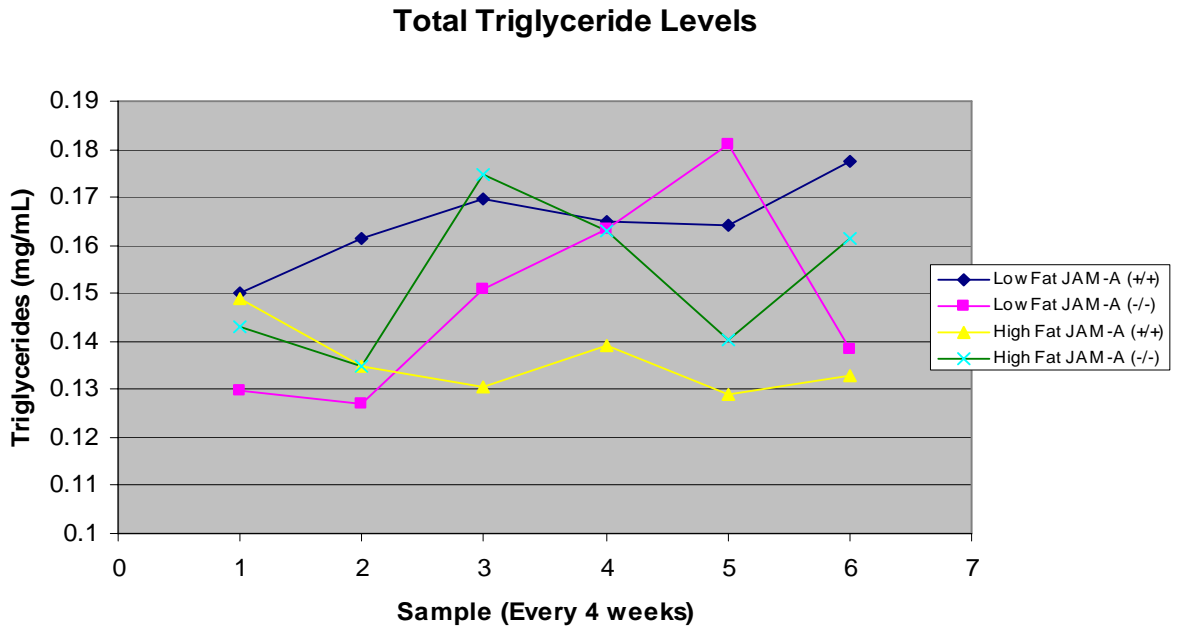


**Figure 15: Total Triglyceride Levels.** Total triglyceride levels derived from blood plasma samples taken once every four weeks via retro-orbital bleeding.



**Figure 16: Physical reaction to diets.** From left to right. Top: two JAM-A (+/+) mice on low fat diet with normal appearance; three JAM-A knock out mice on low fat diet with slightly oily fur and normal weight distribution. Bottom: JAM-A (+/+) mouse on high fat diet exhibiting oily fur, large amount of visceral fat, and some hair loss; three JAM-A knock out mice on high fat diet with oily fur, and some visceral fat.

Physical changes were noted during the duration of the diets. After twelve weeks on the diet, low fat JAM-A (+/+) mice underwent no physical changes in appearance, same with the low fat JAM-A (-/-) mice. Whereas high fat JAM-A (+/+) mice began to develop oily fur shortly before losing most of the fur on the nape of their necks and backs. High fat JAM-A (+/+) mice also began to show visceral weight gain, weight gain focused near the hind legs. High fat JAM-A (-/-) mice also developed oily fur, but did not lose a noticeable amount of hair (Figure 16). They also

gained visceral fat. Most mice developed some scarring of the eyes around fourteen weeks of diet, due to the retro-orbital bleeding.

Categorization of the stage of NAFLD cannot be diagnosed without conducting a liver biopsy (4). Therefore, after twenty-five weeks of experimental diet the mice were sacrificed via carbon monoxide asphyxiation, and cervical dislocation. The fat pads, liver, and kidneys were dissected, weighed, and fixed in 10% formalin. All organs weights were normalized to a percent of total body weight and compared using a two tailed unequal variance t-test, with statistical significance of 0.05 on either tail.

The fat pads are the main storage location of adipocytes in mice. They start near the groin and extend up and back toward the kidneys. The fat pads of the low fat JAM-A (-/-) mice weighed significantly less than the high fat JAM-A (-/-) mice. The liver is located near the stomach and is one of the main filtration systems in the body, involved in glycogen storage, lipid metabolism, and drug detoxification. Low fat JAM-A (+/+) livers were found to be statistically smaller than high fat JAM-A (+/+) livers. Low fat JAM-A (-/-) livers were found to be statistically smaller than the high fat JAM-A (-/-) livers. There was no statistical difference between high fat JAM-A (+/+) livers and high fat JAM-A (-/-) livers. Kidneys also filter the blood, and were therefore examined. Low fat JAM-A (-/-) kidneys were significantly larger than high fat JAM-A (-/-) kidneys. No other variances were statistically determined (Figure 17).

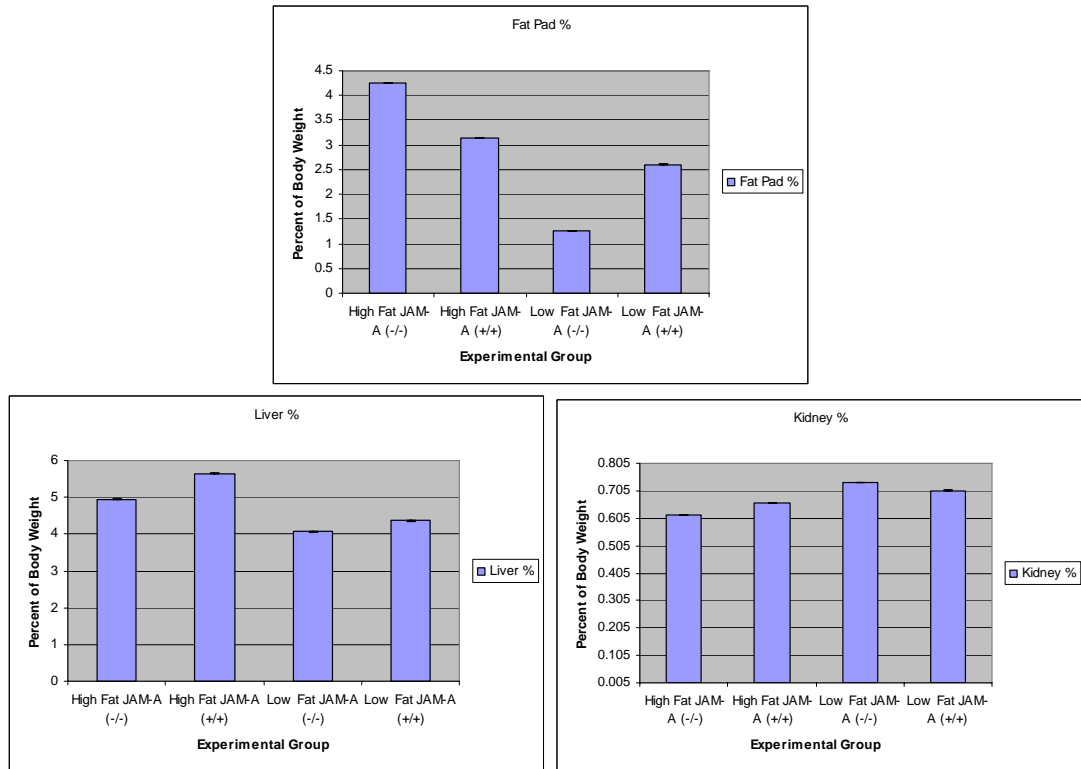


**Figure 17: Organ Weights as a Percentage of the Total Body Weight.** Top: Average visceral fat pad weights as a percentage of the total body weight two-tailed t-test revealed: p-value of 0.038171 between the JAM-A (-/-) groups. Bottom Left: Average liver weights as a percentage of the total body weight, two-tailed t-test revealed: p-value of 0.0166706 between the JAM-A (-/-) groups; p-value of 0.0052026 between the JAM-A (+/+) groups. Bottom Right: Average kidney weights as a percentage of the total body weight, two-tailed t-test revealed: p-value of 0.048624 between the JAM-A (-/-) groups.

After organs were embedded in paraffin, they were sectioned into 8 nm thick sections for staining. Common stains used to identify NAFLD are H&E and Masson's Trichrome. Masson's Trichrome is more popular because it will identify collagen deposits (fibrosis/cirrhosis), a common symptom of advanced NAFLD, in bright blue.

Liver sections stained with Masson's Trichrome revealed that the high fat diet caused physiological changes in the mice. Only one JAM-A (+/+) mouse fed a low fat

diet and one JAM-A (-/-) mouse fed a low fat diet developed small amounts of lipid accumulation in the form of macrosteatosis. Both of the abnormal mice from the low fat groups were female. All other mice from these experimental groups had normal liver histology (Figure 18). JAM-A (+/+) mice on high fat diet developed large amounts of macrovascular steatosis, however, none demonstrated symptoms of NASH. JAM-A (-/-) mice on a high fat diet also developed macrovascular steatosis, but not as severely as the JAM-A (+/+) mice, and some also showed signs of microvascular steatosis (Figure 19).

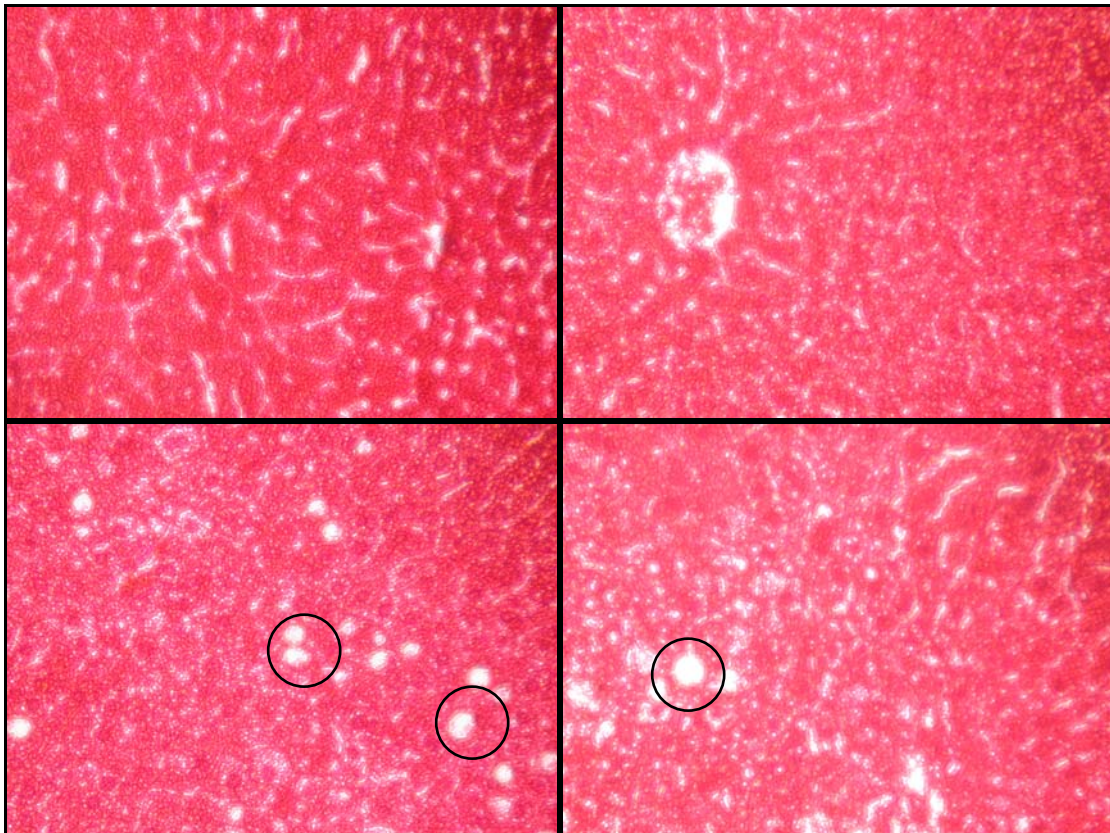


**Figure 18: Hepatitis of Livers – 100X.** Sections stained with Masson's Trichrome. From left to right. Top: liver of JAM-A (+/+) mouse on low fat diet with normal appearance; liver of JAM-A (-/-) mouse on low fat diet with normal appearance. Bottom: liver of a JAM-A (+/+) mouse on high fat diet exhibiting approximately 19 incidences of macrovascular steatosis; liver of a JAM-A (-/-) mouse on high fat diet displaying approximately 6 incidences of macrovascular steatosis. Circled are examples of macrovascular steatosis.

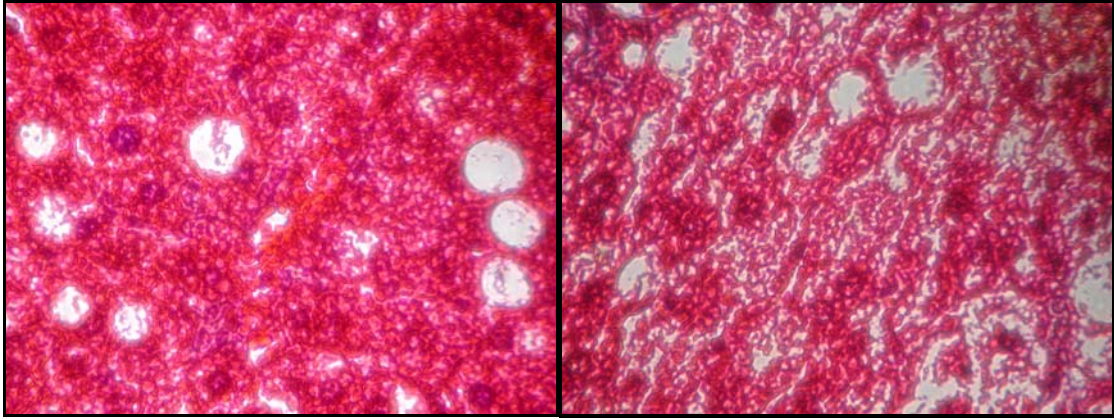


**Figure 19: Hepatitis of Livers – 400X.** Sections stained with Masson's Trichrome. Left: Liver of a JAM-A (+/+) mouse on a high fat diet exhibiting 8 incidences of macrovascular steatosis. Right: Liver of a JAM-A (-/-) mouse on a high fat diet exhibiting approximately 5 incidences of macrovascular steatosis.

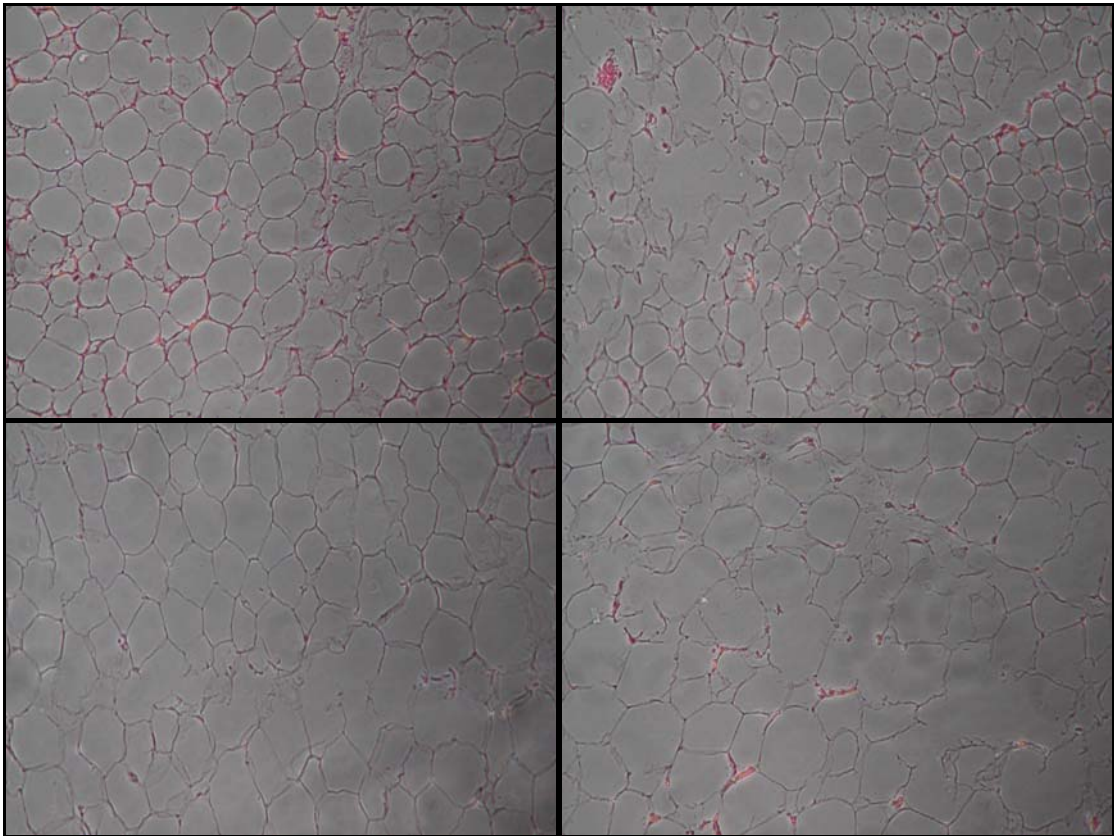


**Figure 20: Histology of Adipocytes Stained with H&E – 100X.** Sections stained with H&E. From left to right. Top: fat pads of JAM-A (+/+) mouse on low fat diet; fat pads of JAM-A (-/-) mouse on low fat diet. Bottom: fat pads of a JAM-A (+/+) mouse on high fat diet; fat pads of a JAM-A (-/-) mouse on high fat diet.

Fat pad sections were stained with either H&E or Oil Red O. H&E stained slides showed the JAM-A (+/+) low fat mice and the JAM-A (-/-) mice on a low fat diet as having adipocytes of approximately the same size. Both high fat diet groups had, on average, larger adipocytes than the low fat diet groups with JAM-A (-/-) mice displaying slightly larger adipocytes than the JAM-A (+/+) mice (Figure 20). A smaller sample size of slides was stained with Oil Red O, and the stain did not behave as expected. The Oil Red O slides showed a similar trend as those stained with H&E. However, the low fat JAM-A (+/+), low fat JAM-A (-/-), and high fat JAM-A (+/+) adipocytes were all approximately the same size. The JAM-A (-/-) adipocytes appear to be larger than the other experimental groups (Figure 21). In today's world, the sharing of results is as important as it is necessary. Therefore, with the help of Dr. Liao's BioInformatics lab, a website was created to allow users dynamically search through a database containing all the sectioning data. The site can be found at <http://128.4.133.57/cgi-bin/search-db.cgi>. Features of the website include: image storage, cross-referenced data for advanced searches, and on-the-fly annotation of sectioning data.

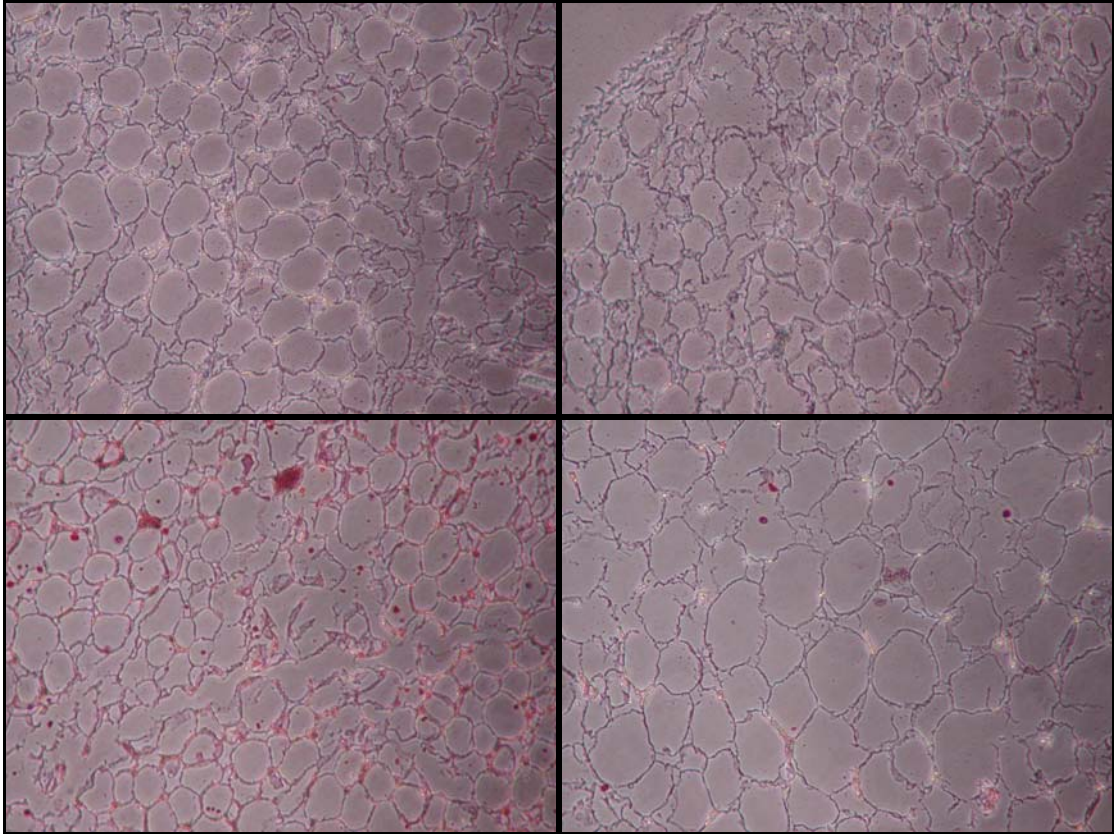


**Figure 21: Histology of Adipocytes Stained with Oil Red O – 100X.** Sections stained with H&E. From left to right. Top: fat pads of JAM-A (+/+) mouse on low fat diet; fat pads of JAM-A (-/-) mouse on low fat diet. Bottom: fat pads of a JAM-A (+/+) mouse on high fat diet; fat pads of a JAM-A (-/-) mouse on high fat diet.

## Chapter 4

### DISCUSSION

Acute inflammatory response is a reaction of the immune system to tissue injury, cellular stress, and systemic inflammation. The normal function of acute inflammatory response includes recruitment of neutrophils and other phagocytic leukocytes to the site of distress that proceed to promote apoptosis and phagocytize any remaining debris. However, recent research combining the work from a variety of disciplines suggests that prolonged weight gain and obesity may cause a continuous inflammatory response damaging, instead of protecting, affected organs. Two methods for researching liver pathological progression have demonstrated in the literature. The first method uses genetically prone rodents such as the Zucker fatty (fa/fa) rat and the leptin-deficient obese ( $Lep^{ob}/Lep^{ob}$ ) mouse that is prone to obesity with little experimental influence. The second method for researching liver disease involves an animal with a genetic variation and a long-term high fat diet (34). Inducing weight gain simulates the progression of obesity in humans, therefore, is preferred to using genetically prone mice.

Another dilemma in preparing experimental conditions to study steatosis of the liver is developing the diet. Most papers mention the use of a “Western style” diet, or a diet where the majority of the caloric intake is comprised of fats. The “Western

style” diet has been poorly defined in papers, listed as both a percentage of composition and a percentage of total caloric intake; this needs to be established before reports on the effects of a “Western style” or high fat diet can be compared. Our diets, high fat including 35.9% fat (wt/wt) and low fat including 4.9% fat (wt/wt), were based off a paper by Surwit et. al, who clearly defined the composition of each of the diets.

Liver and adipocyte histology is studied on either a short term, 11 days to 3 week period, or in long term studies, 12 weeks or longer. Certain breeds of control mice, such as C57BL/6J mice have a natural tendency to gain weight as they age. However, the JAM-A (-/-) mice used were in the process of being back crossed with the C57BL/6 mice and may not yet model the pure strain. Therefore, our diet was administered for a period of 25 weeks to ensure that the diet induced physiological effects. Beginning after five weeks of diet administration, significant variance between the control, JAM-A (+/+) mice on a low fat diet, and the JAM-A (-/-) mice on high and low fat diets emerged. By the end of the diet administration there was an average of 10 grams and 23% weight gain difference between the two JAM-A (-/-) groups. Also, in the high fat diet groups the males gained significantly more weight than the female mice. Previous work in ICAM, another member of the IgSF, deficient mice showed a similar weight gain in the null mice as the JAM-A (-/-) mice, but an greater weight gain in female ICAM null mice over the male ICAM null mice (35). However, multiple studies have both agreed and disagreed with these findings, and the

findings of any one lab are yet to be verified. Until a standardized wild-type bred of mouse, diet, and longevity of experiment exists, more confusion will unravel in future. For now, only studies conducted using the same dietary conditions and mice can be compared to each other. For this experiment mice were fed *ad libitum*; however, in the future the caloric intake of the mice should be monitored.

Every four weeks of experimentation blood samples were drawn via retro-orbital sinus puncture after a fourteen-hour fast. The blood from mice in the same experimental group was pooled in a K<sub>2</sub>EDTA lined tube to prevent coagulation and centrifuged at 3000rpm for five minutes to isolate the blood plasma. During normal, non-fasted conditions, cholesterol and triglycerides are trafficked back and forth from the hepatocytes and adipocytes in the process of lipid metabolism and storage. Mice are fasted before drawing blood so that the amount of free-floating triglycerides and cholesterol can be measured without interference from triglyceride trafficking molecules. Mice on a high fat diet would be expected to have more free-floating cholesterol and triglycerides because the hepatocytes would be overwhelmed with lipid metabolism and the fat pads would not be able to create adipocytes quickly enough to store the excess. In addition, mice lacking JAM-A should have reduced control over the tight junctions and increased transendothelial migration of a variety of molecules such as cholesterol. When comparing experimental groups, the control group cholesterol levels are used to establish normal, healthy levels of these molecules, since there is too much variation between species to establish healthy

levels. Based on the low fat JAM-A (+/+) mice, high fat JAM-A (-/-) mice were in the unhealthy range for total cholesterol, HDL-cholesterol, and LDL-cholesterol while high fat JAM-A (+/+) mice remained in the healthy zone. This trend in cholesterol levels supports our theory that JAM-A's tight junction function has some control mechanism on the flow of cholesterol in the blood. However, no trend was seen in the triglyceride levels.

Lipid influx into the adipocytes and liver causes inflammatory responses via the release of CXC chemokines. Once neutrophils and macrophages reach the site of inflammation, they attempt to alleviate the symptoms by inducing apoptosis in inflamed cells, further agitating the immune response. Since livers undergo regeneration when injured, mice exposed to larger amounts of immune-stimulating factors, mainly a high fat diet, should be expected to have increased liver regeneration caused by oxidative damage to the liver. In addition, when exposed to large amounts of lipids, fat pads undergo increased adipogenesis. Therefore, mice on low fat diets should not experience an immune reaction, no steatosis induced liver regeneration should occur, and livers will be of a normal size. However, in mice on a high fat diet, the livers should be larger due to an increase in mediators of an immune response. Mice on low fat diets should also maintain smaller fat pads than mice on high fat diets. If JAM-A does regulate the passage of triglycerides, then increased amounts of lipids should enter the fat pads, which would induce adipogenesis and lead to larger fat pads. Based on liver sectioning, livers of low fat JAM-A (-/-) mice weighed significantly

less than the livers of high fat JAM-A (-/-) mice. There is no significant difference between the two low fat diet groups, or the two high fat diet groups. Therefore there was a difference based on diet, but no discernable effect of JAM-A on MES fat pad size. Liver weights showed a similar trend with a difference between the diet groups but not between the JAM-A (-/-) and JAM-A (+/+) mice. Other researchers have weighed other regions of fat, including subcutaneous fat pads (ING), retroperitoneal fat pads, epididymal fat pads, and brown fat pads (32, 36), that should be included in future studies to gain a complete insight into the distribution of lipids in JAM-A null mice fed a high fat diet.

Despite the growing capabilities of ultrasonic scanning techniques, the gold standard of NAFLD classification continues to be the liver biopsy. If JAM-A is signaled to assist in recruitment of neutrophils through the tight junction, then JAM-A (+/+) mice on a high fat diet will display a higher incidence of steatosis than JAM-A (-/-) mice. As predicted, the majority of JAM-A (+/+) mice and JAM-A (-/-) mice on low fat diets did not show any signs of steatosis. One JAM-A (+/+) and one JAM-A (-/-) mouse in the low fat diet group showed signs of steatosis (not shown), but was explained as being genetically influenced. JAM-A (-/-) mice on a high fat diet showed large amounts of macrovascular steatosis and some signs of microvascular steatosis, but JAM-A (+/+) mice on a high fat diet had a higher prevalence of macrovascular steatosis. Macrovascular steatosis is the precursor to NASH, and therefore, high incidence of macrovascular steatosis indicates a worse NAFLD prognosis.

Sections of MES fat pads were analyzed using H&E staining. Some reports of macrophages in the adipocytes have been referred to as a cause of inflammation in the fat pads (37). If macrophages do enter the fat pads and inflame adipocytes, then the fat pad sections should follow the same trend as the liver histology sections. Low fat JAM-A (+/+) mice and low fat JAM-A (-/-) mice both have similarly sized adipocytes in their fat pads. Contrast to these groups, the JAM-A (+/+) high fat and JAM-A (-/-) high fat mice both have larger adipocytes. Further analysis is necessary to determine whether the adipocytes from JAM-A (+/+) high fat mice are larger than the adipocytes from the JAM-A (-/-) high fat mice, but visually there appears to be larger adipocytes in the JAM-A (-/-) mice.

Overall, the results indicate that JAM-A plays a role in the progression of NAFLD and adipocyte generation. Further analysis of JAM-A's role, including a complete analysis of all forms of fat, monitored food intake, body mass index, and microarray determination of upregulated genes is necessary to further classify JAM-A's specific function. Obesity is a growing trend in many countries, with the worst incidence in the United States, and its role in NAFLD needs to be taken seriously. Since JAM-A affects the extravasation of neutrophils, but not to the same extent as ICAM-1, JAM-A may eventually be used as a drug target to modulate the effects of lipids in NAFLD without eliminating normal leukocyte inflammatory response.

## References

1. DeAngelis, R. A., Markiewski, M. M., Taub, R., & Lambris, J. D. (2005) *Hepatology* **42**, 1148-1157.
2. Brody, J. E. (2005) in *The New York Times*.
3. Zakim, D. B., Thomas (2003) *Hepatology* (Saunders, Philadelphia).
4. Saito, T., Misawa, K., & Kawata, S. (2007) *Internal medicine (Tokyo, Japan)* **46**, 101-103.
5. Farrell, G. C. & Larter, C. Z. (2006) *Hepatology* **43**, S99-S112.
6. Nanda, K. (2004) *Pediatr Transplant* **8**, 613-618.
7. Salt, W. B., 2nd (2004) *Journal of insurance medicine (New York, N.Y)* **36**, 27-41.
8. Yang, S., Lin, H. Z., Hwang, J., Chacko, V. P., & Diehl, A. M. (2001) *Cancer Res* **61**, 5016-5023.
9. Lindor, K. D. (2001) (American Liver Foundation).
10. Chow, J. H. C., Cheryl (2006) *The Encyclopedia of Hepatitis and Other Liver Diseases* (Infobase Publishing, New York).
11. Okita, K. (2005) *NASH and Nutritional Therapy* (Springer, Tokyo).
12. Poordad, F. F. (2005) *Expert Opin Emerg Drugs* **10**, 661-670.
13. Beller, M., Riedel, D., Jansch, L., Dieterich, G., Wehland, J., Jackle, H., & Kuhnlein, R. P. (2006) *Mol Cell Proteomics* **5**, 1082-1094.
14. Bacon, B. R., Farahvash, M. J., Janney, C. G., & Neuschwander-Tetri, B. A. (1994) *Gastroenterology* **107**, 1103-1109.
15. Jaeschke, H., Gores, G. J., Cederbaum, A. I., Hinson, J. A., Pessayre, D., & Lemasters, J. J. (2002) *Toxicol Sci* **65**, 166-176.
16. Jaeschke, H. (2006) *American journal of physiology* **290**, G1083-1088.
17. Lodish, H. B., Arnold; Matsudaira, Paul; Kaiser, Chris; Krieger, Monty; Scott, Matthew; Zipursky, Lawrence; and Darnell, James (2003) *Molecular Cell Biology* (W.H. Freeman and Company, New York).
18. Karp, G. (2005) *Cell and Molecular Biology: Concepts and Experiments* (John Wiley & Sons, Inc., San Diego).
19. Jaeschke, H. & Hasegawa, T. (2006) *Liver Int* **26**, 912-919.
20. Liu, L. & Kubes, P. (2003) *Thromb Haemost* **89**, 213-220.
21. Khandoga, A., Kessler, J. S., Meissner, H., Hanschen, M., Corada, M., Motoike, T., Enders, G., Dejana, E., & Krombach, F. (2005) *Blood* **106**, 725-733.
22. Ebnet, K., Suzuki, A., Ohno, S., & Vestweber, D. (2004) *J Cell Sci* **117**, 19-29.
23. Nourshargh, S., Krombach, F., & Dejana, E. (2006) *J Leukoc Biol* **80**, 714-718.
24. Ostermann, G., Fraemohs, L., Baltus, T., Schober, A., Lietz, M., Zerneck, A., Liehn, E. A., & Weber, C. (2005) *Arteriosclerosis, thrombosis, and vascular biology* **25**, 729-735.
25. Muller, W. A. (2003) *Trends Immunol* **24**, 327-334.

26. Naik, U. P., Naik, M. U., Eckfeld, K., Martin-DeLeon, P., & Spychala, J. (2001) *J Cell Sci* **114**, 539-547.
27. Bazzoni, G. (2003) *Curr Opin Cell Biol* **15**, 525-530.
28. Mandell, K. J. & Parkos, C. A. (2005) *Advanced drug delivery reviews* **57**, 857-867.
29. Ostermann, G., Weber, K. S., Zerneck, A., Schroder, A., & Weber, C. (2002) *Nat Immunol* **3**, 151-158.
30. Martinez-Mier, G., Toledo-Pereyra, L. H., & Ward, P. A. (2000) *The Journal of surgical research* **94**, 185-194.
31. Cooke, V. G., Naik, M. U., & Naik, U. P. (2006) *Arteriosclerosis, thrombosis, and vascular biology* **26**, 2005-2011.
32. Surwit, R. S., Feinglos, M. N., Rodin, J., Sutherland, A., Petro, A. E., Opara, E. C., Kuhn, C. M., & Rebuffe-Scrive, M. (1995) *Metabolism* **44**, 645-651.
33. Gerdes, L. U., Gerdes, C., Klausen, I. C., & Faergeman, O. (1992) *Clinica chimica acta; international journal of clinical chemistry* **205**, 1-9.
34. Kim, S., Sohn, I., Ahn, J. I., Lee, K. H., Lee, Y. S., & Lee, Y. S. (2004) *Gene* **340**, 99-109.
35. Dong, Z. M., Gutierrez-Ramos, J. C., Coxon, A., Mayadas, T. N., & Wagner, D. D. (1997) *Proceedings of the National Academy of Sciences of the United States of America* **94**, 7526-7530.
36. Gregoire, F. M., Zhang, Q., Smith, S. J., Tong, C., Ross, D., Lopez, H., & West, D. B. (2002) *Am J Physiol Endocrinol Metab* **282**, E703-713.
37. Robker, R. L., Collins, R. G., Beaudet, A. L., Mersmann, H. J., & Smith, C. W. (2004) *Obes Res* **12**, 936-940.